



OPEN Exploring the potential mechanisms of anti-pulmonary fibrosis effects of Luo Han Guo via network pharmacology, molecular docking, and experimental validation

Qinlin Cui^{1,2}, Yingyi Liu^{1,2}, Yuxuan Li¹, Zhan Li¹, Wencai Wei¹, Simei Yang¹, Xin Liu¹, Lei Chen¹, Kunyu Xu¹, Yihan Li¹, Qingbi Zhang¹✉ & Jun Bai¹✉

Idiopathic pulmonary fibrosis (IPF) is a chronic interstitial lung condition distinguished by a complex etiology, poor prognosis and exhibiting high mortality rates. While therapeutic drugs are currently available, they often come with notable side effects. Luo Han Guo (LHG), a medicinal plant, is known for its properties in moistening the lungs, relieving cough, calming asthma, and resolving phlegm; however, systematic research on its potential therapeutic mechanisms and active ingredients for IPF is lacking. This study utilized network pharmacology to predict the active ingredients, key targets, and potential mechanisms of LHG's anti-IPF effects, followed by molecular docking simulations of the active ingredients and their potential targets, which were subsequently validated through in vivo experiments. From 91 potential targets of LHG, four key targets were identified. Analysis of the compound-target network diagram suggested that kaempferol, 11-oxomogrosin V, and Mogrol may be the principal active compounds of LHG for treating IPF. Additionally, KEGG pathway enrichment analysis indicated that LHG might mitigate IPF through the PI3K/AKT and SRC/STAT3 pathways. In conclusion, this study provides preliminary insights into the active constituents and possible molecular mechanisms of LHG in alleviating IPF, offering a novel perspective for investigating the pharmacological effects of LHG in IPF treatment.

Keywords Idiopathic pulmonary fibrosis, Luo Han Guo, Network pharmacology, *Siraitia grosvenorii*

Abbreviations

IPF	Idiopathic pulmonary fibrosis
COPD	Chronic obstructive pulmonary disease
CSE	Cigarette smoke extract
LPS	Lipopolysaccharide
PM ₁₀	Particulate matter 10
LHG	Luo Han Guo
SDF	Structural data files
BLM	Bleomycin
α-SMA	α-Smooth muscle actin
Col-I	Collagen type I
NSCLC	Non-small cell lung cancer
RPF	Renshen pingfei formula
AMPK	Adenosine 5'-monophosphate (AMP)-activated protein kinase
Nrf2	Nuclear factor erythroid 2-related factor-2

¹Environmental Health Effects and Risk Assessment Key Laboratory of Luzhou, School of Public Health, Southwest Medical University, Luzhou 646000, China. ²Qinlin Cui and Yingyi Liu these authors have contributed equally to this work. ✉email: qingbizhang@126.com; baijun@swmu.edu.cn

TPA	12-O-Tetradecanoylphorbol-13-acetate
EBV	Epstein-barr virus
PI3K	Phosphoinositide 3-kinase
AKT	Protein kinase B
EGFR	Epidermal growth factor receptor
GO	Gene ontology
KEGG	Kyoto encyclopedia of genes and genomes
PPI	Protein and protein interaction
ECL	Enhanced chemiluminescence
TCMSP	Traditional Chinese medicine systems pharmacology database

Interstitial lung disease, recognized as a type of idiopathic interstitial pneumonia, is typified by widespread inflammation of the lung parenchyma and alveoli, accompanied by interstitial fibrosis. Among its forms, idiopathic pulmonary fibrosis (IPF) is notably prevalent, marked by chronic and progressively worsening fibrosis within the pulmonary interstitium, and is characterized by symptoms such as breathlessness, coughing, and a gradual decline in pulmonary function^{1,2}. For IPF patients, respiratory failure remains the leading cause of mortality, primarily affecting older individuals, with an average survival time of around 3 to 4 years post-diagnosis³. Risk factors that are widely associated with IPF include environmental exposures, smoking, and viral infections. Furthermore, various cellular mechanisms like apoptosis, epithelial-mesenchymal transition, oxidative stress, and mitochondrial dysfunction contribute significantly to the initiation and progression of IPF⁴. New pharmacological treatments, such as nitidafil and pirfenidone, have been developed to target IPF and have shown effectiveness in improving patient conditions. Nonetheless, these medications are costly, often induce adverse reactions—mainly affecting the skin and digestive systems^{5,6}—and are frequently poorly tolerated by patients⁷. Therefore, a pressing need exists for treatments that are both safer and more economical. Luo Han Guo, a traditional Chinese medicinal plant, offers a potential alternative.

Luo Han Guo (*Siraitia grosvenorii*, Cucurbitaceae family) is a natural sweetener with documented lung-relieving, cough-relieving, and laxative efficacy⁸. In traditional Chinese medicine, it is employed to treat respiratory conditions, including cough and asthma⁹. Luo Han Guo extract exhibits a range of medicinal properties, including antioxidant effects through scavenging of peroxy radicals¹⁰, neuroprotective effects¹¹, and potential antibacterial activity¹². Emerging studies also demonstrate its respiratory benefits, as it alleviates inflammatory responses and reduces tissue damage in models of chronic obstructive pulmonary disease (COPD) induced by exposure to cigarette smoke extract (CSE) and lipopolysaccharide (LPS)¹³. The extract also diminishes inflammation induced by particulate matter 10 (PM₁₀) and diesel exhaust through the inhibition of the MAPK/NF- κ B pathway¹⁴. Experiments show that treatment with LHG extract can significantly reduce the area of collagen fibers in bleomycin-induced lung injury, alleviate inflammatory responses, and inhibit the increased expression of α -SMA (alpha-smooth muscle actin) and COL I (collagen type I) proteins caused by bleomycin¹⁵. Furthermore, a water-extracted residual fraction of Luo Han Guo has shown anti-inflammatory properties, as noted in research by Yoon-Young Sung and colleagues, where this extract suppressed the expression of IL-13, TARC, MUC5AC, TNF- α , and IL-17 in an ovalbumin-stimulated mouse model of asthma, thus exhibiting anti-asthmatic potential¹⁶. These findings support the potential application of Luo Han Guo extract in treating lung conditions. However, the specific pharmacological pathways of Luo Han Guo extract (LHG) in IPF treatment remain largely unexplored. Given its various bioactive components, identifying the precise mechanisms of action of LHG poses significant challenges, necessitating new research approaches to pinpoint its active ingredients and their molecular functions in IPF therapy.

Network pharmacology, as a systems biology method, employs network analysis to elucidate disease processes and interactions between drugs and biological systems, thus playing an essential role in new drug discovery¹⁷. It can screen drug active ingredients and identify their targets, and through constructing “compound–target” or “protein–protein” networks, complex relationships between biological systems, drugs, and diseases can be characterized¹⁸. Molecular docking, a computational method, is widely used to predict the binding interactions between a protein and a ligand, such as a small molecule drug, aiming to find the ligand’s optimal binding configuration within the protein’s active site, which is crucial for assessing the potential biological activity of small molecules¹⁹.

This study utilized network pharmacology, molecular docking, and experimental research methods to identify active compounds and key targets for IPF alleviation by LHG. We conducted preliminary validation using a rat IPF model to lay the foundation for further research. The workflow is shown in Fig. 1.

Materials and methods

Network pharmacology analysis

Identification of active ingredients and targets in LHG

To explore potential bioactive components in Luo Han Guo (LHG), the Traditional Chinese Medicine Systems Pharmacology database (<https://tcmospw.com/tcmosp.php>) was accessed, and additional insights were gathered from related literature. Chemical structures and SMILES representations of the active ingredients were retrieved from PubChem (<https://pubchem.ncbi.nlm.nih.gov/>) and then processed through the SwissTargetPrediction platform (<http://www.swisstargetprediction.ch/>) to predict biological targets. The UniProt database (<https://www.uniprot.org/>) was employed for the standardization of gene nomenclature.

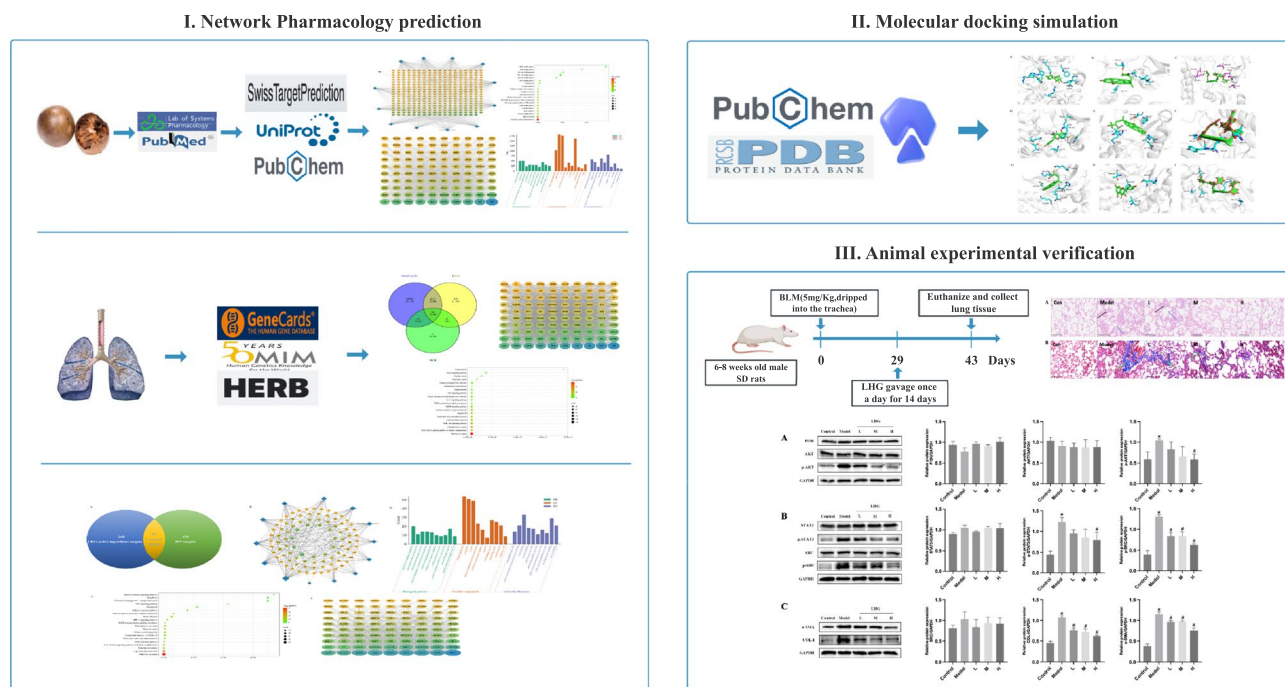


Fig. 1. Lines of work of this study.

Collection of IPF-related genes

The GeneCards database (<https://www.genecards.org/>), the OMIO database (<https://www.omim.org/>), and the HERB database (<http://herb.ac.cn/>) were utilized to retrieve genes associated with IPF. The intersection of all acquired genes was considered as candidate genes.

Construction of an active ingredients-target network

Cytoscape 3.9.1 (<http://www.cytoscape.org/>) software was utilized to construct an interactive network connecting ingredients to targets. The nodes represented the active ingredient, targets, and the edges represented the interaction between nodes.

Network of protein Interactions

The active ingredient targets of LHG or candidate genes for IPF are imported into the STRING database (<http://cn.string-db.org/>) to construct a PPI network. The PPI network is then visualized using Cytoscape 3.9.1 software.

GO function enrichment analysis and KEGG pathway enrichment analysis of targets

GO functional analysis and KEGG pathway analysis were performed using the DAVID database (<https://david.ncicrf.gov/>). Input Data: A list of genes to be analyzed was provided. Enrichment Calculation: Statistical methods were used to compute the enrichment level of each GO term within the target genes, evaluating whether it was significantly higher than the random distribution in the background gene set. Additionally, statistical calculations were performed to assess the enrichment significance of each KEGG pathway in the target genes, generating p-values. Multiple Testing Correction: Given the large number of tests, the original p-values were adjusted using the FDR (False Discovery Rate) method to control the false positive rate.

Significance Threshold: A corrected p-value (FDR) < 0.05 was set as the threshold, indicating that the enrichment of a GO term or KEGG pathway in the target genes was statistically significant. The results were visualized using the Weishengxin platform (<https://www.bioinformatics.com.cn/>).

Molecular docking

First, the protein and ligand structures were obtained. The structures of receptor proteins AKT1 (4EKL), STAT3 (6NUQ), and SRC (2H8H) were retrieved and downloaded from the Protein Data Bank (PDB), and the structure data files (SDF format) of ligands were obtained from the PubChem database. Next, protein structure preprocessing was performed. The protein structure files were opened with PyMOL, the sequences were displayed, ligand molecules and water molecules were removed, and the processed structures were saved as new PDB files. Then, ligand structure preprocessing was carried out, converting the ligand SDF files to PDB format using Open Babel 3.0.1 (<https://openbabel.org/>) software. Hydrogen atoms were added to both the protein and ligand, which were saved as PDBQT files. Finally, molecular docking was performed: the parameters of the docking box and docking (with the number of runs set to 50) were set, the optimal binding conformation was

obtained through operation, and the corresponding energy score was calculated. The docking structure files were exported, and the results were visually analyzed using PyMOL.

Experimental validation

Preparation of LHG extract

The dried Luo Han Guo was washed and soaked in water for 30 min at a material-to-liquid ratio of 1:15 (g/mL), followed by boiling for 40 min, three times in total. The aqueous extract was filtered through gauze, concentrated to 1L using a rotary evaporator, and stored in a refrigerator at $-80\text{ }^{\circ}\text{C}$ overnight. It was then freeze-dried using a lyophilizer, and the resulting product was stored at $4\text{ }^{\circ}\text{C}$ for future use. The residue of Luo Han Guo after water extraction was collected, dried, and powdered using a pulverizer. Using 80% ethanol as the solvent (material-to-liquid ratio 1:25), ultrasonic extraction was carried out at 400W power and $45\text{ }^{\circ}\text{C}$ for 14 min. The mixture was centrifuged at high speed, filtered, and finally freeze-dried, and stored at $4\text{ }^{\circ}\text{C}$. The two freeze-dried products were mixed and orally administered to rats.

Animal experiments

Healthy male SPF-grade SD rats (6–8 weeks old) were obtained from Beijing Specific Biological Company (Certificate No.: SCXK (Beijing) 2019–0010) and housed in Southwest Medical University's SPF animal laboratory (License SYXK (Chuan) 2023–0065). The rats had unrestricted access to food and water under controlled conditions ($25 \pm 1\text{ }^{\circ}\text{C}$, $50 \pm 5\%$ humidity, 12-h light/dark cycle).

After a week of acclimatization, forty male SD rats were randomly assigned to five groups: control group, BLM plus saline group, BLM plus low-dose LHG group (25 mg/kg), BLM plus medium-dose LHG group (50 mg/kg), and BLM plus high-dose LHG group (100 mg/kg). On day 0, the pulmonary fibrosis model was established using a BLM dose of 5 mg/kg via non-exposed endotracheal drip, while the control group received an equivalent volume of saline via the same method. Suspensions at various concentrations were formulated by dissolving Luo Han Guo extract in a 0.5% sodium carboxymethyl cellulose solution. The suspensions were administered via gavage to the rats once daily for 14 consecutive days, starting on the 29th day of the study.

This study was approved by the Southwest Medical University committee (Permit SWMU20230078). This study complied with the Regulations on the Management of Laboratory Animals issued by the National Science. All procedures were performed in accordance with the ethical standards of the Guide for the Care and Use of Laboratory Animals published by the National Institutes of Health and ARRIVE guidelines.

Sample collection

Anesthesia was induced in the rats using 2% sodium pentobarbital at 50 mg/kg. The chest wall was cut open to expose the thoracic cavity, and cardiac perfusion was performed with saline after collecting blood from the heart to prevent blood residues in the lung tissue from affecting subsequent experimental results. Portions of the lung tissue were collected, rinsed with 0.9% saline, and stored at $-80\text{ }^{\circ}\text{C}$ for later use. The remaining lung tissue was fixed in paraformaldehyde for further experiments.

HE and Masson staining of lung tissue

The left lung tissue samples were fixed in 4% paraformaldehyde, followed by dehydration in 75%, 85%, 95%, and 100% ethanol. The samples were embedded in paraffin, sectioned into 3–4 μm slices, deparaffinized, and stained with hematoxylin, eosin, and Masson's trichrome before sealing with neutral resin for microscopic examination.

Western blot

Total proteins were extracted from the lung tissues, and concentrations were quantified. Equal amounts of protein were separated via 10% SDS-PAGE and transferred to PVDF membranes, which were blocked and then incubated overnight at $4\text{ }^{\circ}\text{C}$ with primary antibodies. Following secondary antibody incubation for 1 h at room temperature, bands were exposed with an ECL kit and quantified using Image J 1.54f. (Image Processing and Analysis in Java, <https://imagej.nih.gov/ij/>) software, with GAPDH as the internal reference.

Statistical analysis

All experimental data were analyzed using GraphPad Prism 8.0. Results are presented as mean \pm standard deviation. One-way ANOVA was employed to compare the means of different groups, followed by Student–Newman–Keuls test for multiple comparisons. Results were considered significant at $P < 0.05$.

Results

Targets of LHG active ingredients

TCMSP (Traditional Chinese Medicine Systems Pharmacology) is a widely used database in the field of traditional Chinese medicine. It integrates herb-compound-target-disease networks, making it particularly suitable for analyzing complex systems like LHG. Through TCMSP, compounds with bioavailability $\geq 30\%$ and drug-likeness ≥ 0.18 are identified as active ingredients. Bioavailability $\geq 30\%$ serves as the empirical threshold for “bioavailable and functional” in drug development, while drug-likeness ≥ 0.18 incorporates structural characteristics of traditional herbal medicine components to avoid excluding potentially active ingredients. Additionally, the active ingredients of LHG were supplemented based on relevant literature. These compounds' potential targets were predicted using Swiss Target Prediction. After filtering out unreliable targets and duplicates, as shown in Fig. 2A a total of 430 potential targets for LHG active ingredients corresponding to 13 bioactive compounds were identified. Using Cytoscape 3.9.1, a compound-target network was created where the most significant compounds identified included Kaempferol, Mogrol, Beta-sitosterol, Flazin, and ZINC03860434, with respective target counts of 97, 89, 85, 83, and 80. These targets were subsequently input into in the STRING

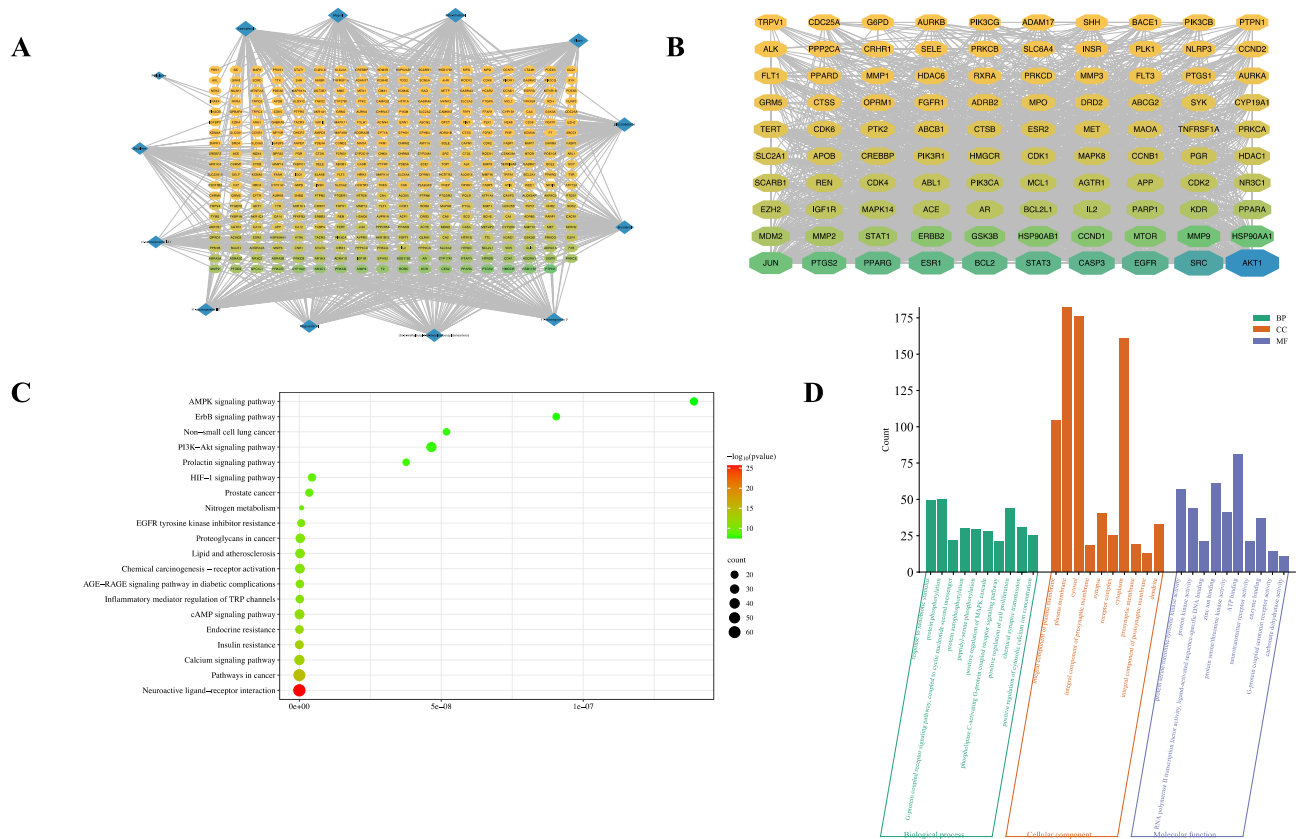


Fig. 2. Network pharmacological analysis of LHG active compound targets. **(A)** LHG active ingredient-target network. **(B)** Protein networks of the top 100 targets. **(C, D)** KEGG pathway enrichment analysis and GO enrichment analysis of LHG targets.

database, leading to the construction of a PPI network, focusing on the top 100 targets ranked by their degree value (Fig. 2B). Components with high Degree values (e.g., kaempferol) correspond to more targets, suggesting they may be core active ingredients; Targets with high Degree values (e.g., AKT1) serve as common nodes for multiple components and should be prioritized as key targets for validation. According to the literature, several of the top 20 targets, including SRC, AKT1, STAT3, HS90AA1, ESR1, and PIK3R1, play crucial roles in the progression of IPF. KEGG pathway enrichment revealed significant enrichment in 183 pathways, with the top 20 pathways identified (Fig. 2C). These pathways primarily included “Pathways in Cancer,” “EGFR Tyrosine Kinase Inhibitor Resistance,” “cAMP Signaling Pathway,” “Chemical Carcinogenesis-Receptor Activation,” and the “PI3K-AKT Signaling Pathway.” The GO analysis (Fig. 2D) revealed that these targets are involved in response to xenobiotic stimulus, protein phosphorylation, extracellular exosome formation, receptor complexes, and protein kinase activity. Collectively, these findings suggest that LHG contains multiple bioactive compounds that target a variety of proteins associated with different biological activities, potentially serving as candidates for the treatment of IPF.

Analyzing the function of IPF-related genes

By searching for “pulmonary fibrosis” in GeneCards, OMIM, and HERB databases, we identified 720 IPF-related genes (Fig. 3A). KEGG pathway enrichment analysis showed that 173 pathways were enriched, the top 20 KEGG analysis results included key pathways such as Pathways in Cancer, PI3K-Akt Signaling Pathway, EGFR Tyrosine Kinase Inhibitor Resistance, TNF Signaling Pathway, Cytokine-Cytokine Receptor Interaction, and “MAPK Signaling Pathway (Fig. 3B). Based on degree values, the top 100 IPF-related genes were selected, with key genes including AKT1, SRC, STAT3, and EGFR, as shown in Fig. 3C. Interestingly, LHG active compounds share functional pathways with IPF-related genes, these key genes have been reported in the IPF literature to regulate fibrosis, hinting at a possible impact of LHG on IPF progression via these pathways.

Cross-analysis of LHG active ingredients targets with IPF-related genes

The LHG active ingredients targets and IPF target genes were entered into the online Venny 2.1 platform for Venn analysis, resulting in 91 intersecting targets (Fig. 4A). Next, the LHG active ingredients-targets network map (Fig. 4B) was constructed. The results showed that the LHG active ingredients targeting the most IPF-associated proteins were ZINC03860434, Flazin, Kaempferol, 11-oxomogroside V, and Mogrol, with 30, 27, 25, 21, and 20 targets, respectively. KEGG analysis of these 91 intersecting targets highlighted Pathways in Cancer, TNF Signaling Pathway, EGFR Tyrosine Kinase Inhibitor Resistance, ErbB Signaling Pathway, and Lipid and

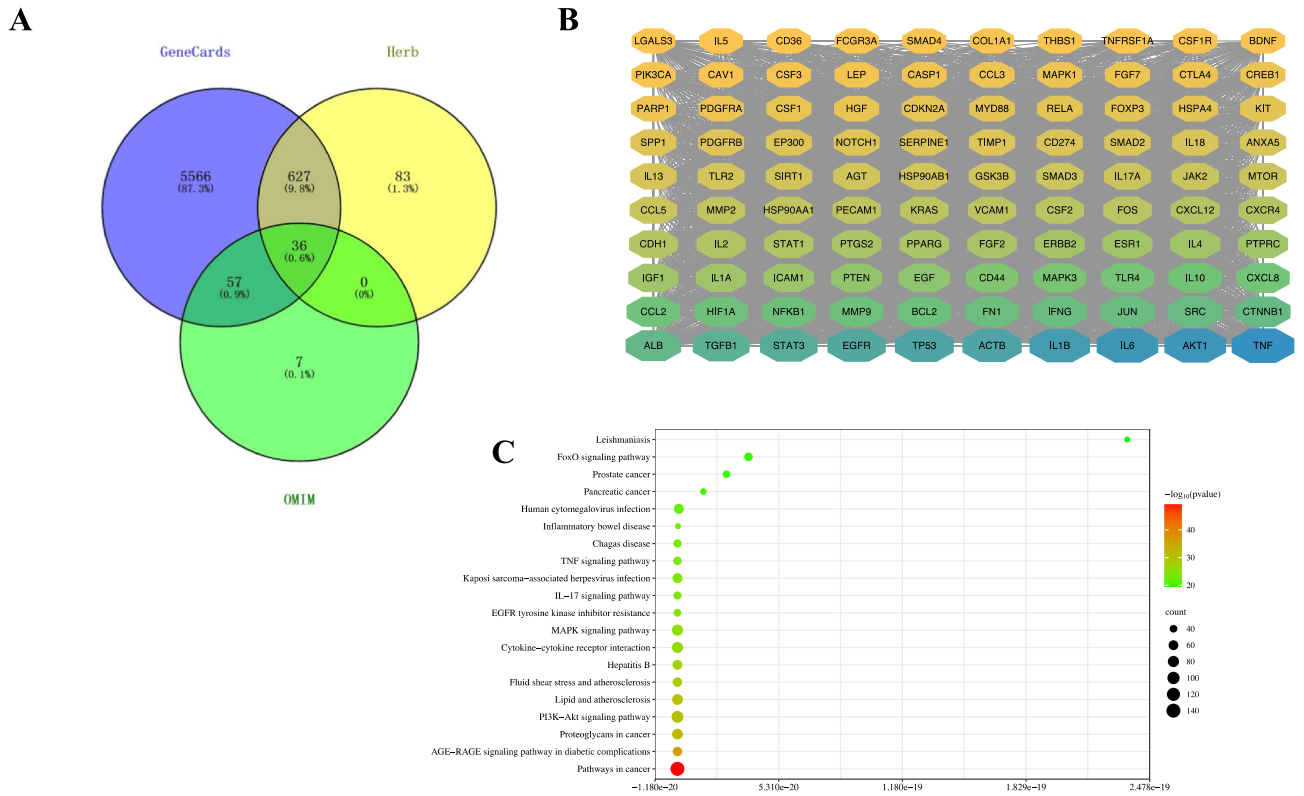


Fig. 3. Network pharmacological analysis of genes related to IPF. **(A)** A total of 720 IPF-related genes. **(B)** KEGG pathway enrichment analysis of IPF-related genes (the top 20 pathways). **(C)** PPI network.

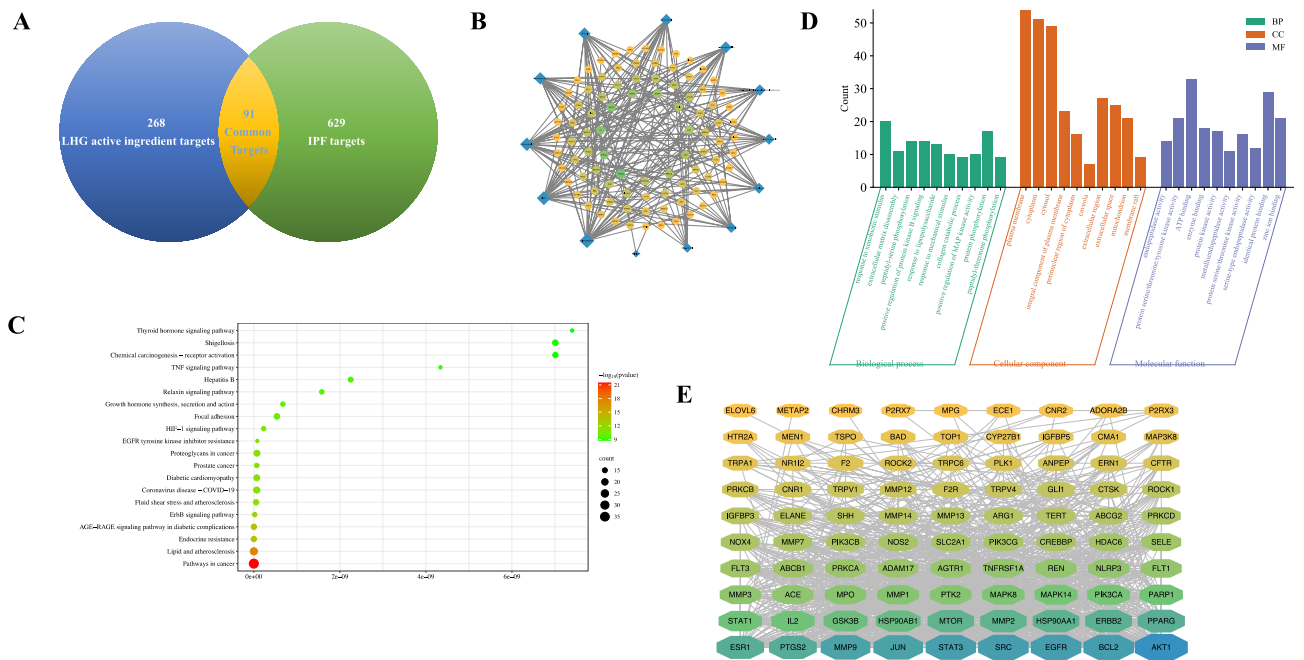


Fig. 4. Comprehensive analysis of LHG active ingredients targets and IPF-related genes. **(A)** The Venn diagram displays the intersecting targets. **(B)** Construction of active ingredients-intersecting targets networks. **(C)** KEGG pathway enrichment analysis and **(D)** GO enrichment analysis. **(E)** PPI network of intersecting targets.

Atherosclerosis (Fig. 4C). Subsequent GO functional enrichment analyses (Fig. 4D) revealed that the targets were primarily involved in inflammatory responses, protein phosphorylation, membrane rafts, and protein kinase activity. Interactions among these targets were further analysed using the STRING database, with data visualized in Cytoscape, building a PPI network, focusing on key genes like TNE, AKT, EGFR, BCL2, STAT3, and SRC (Fig. 4E).

To further explore the important targets of LHG in IPF treatment, we analyzed the targets from three perspectives: (1) Intersecting targets between LHG active ingredients targets and IPF-related genes. (2) The key genes in the PPI Network of the intersecting targets and IPF-Related genes. (3) Targets of LHG active components that play important roles in IPF biological processes or pathways. These analyses showed that STAT3, AKT1, and SRC are key genes involved in the intersecting target PPI network and are key targets for the active ingredients of LHG. Furthermore, the SRC/STAT3 and PI3K/AKT signaling pathways are also associated with resistance to epidermal growth factor receptor tyrosine kinase inhibitors, AKT1, STAT3, and SRC may represent key targets for LHG in IPF therapy. Therefore, in subsequent experiments, phosphorylated forms (p-AKT, p-STAT3, p-SRC) were selected as detection indicators for Western blot to validate pathway activity.

Molecular docking analysis

We predicted the binding abilities of three major active compounds in LHG (Kaempferol, 11-oxomogroside V, and Mogrol) with key targets (AKT1, SRC, and STAT3) through molecular docking. Molecular docking of SRC with Kaempferol (Fig. 5A) revealed hydrogen bonding interactions between Kaempferol and amino acid residues Tyr416, Lys423, Arg388, and Lys295, along with hydrophobic interactions with Phe278. When SRC was docked with Mogrol (Fig. 5B), hydrogen bonding occurred with Thr247, while hydrophobic interactions were observed with Leu161, Ile153, and Val399. Docking of SRC with 11-oxomogroside V (Fig. 5C) showed that 11-oxomogroside V hydrogen bond interactions with amino acid residues His319, Lys401, Asn135, Tyr90 and Gln144, and hydrophobic interaction with Glu147. In the docking of AKT1 with Kaempferol,

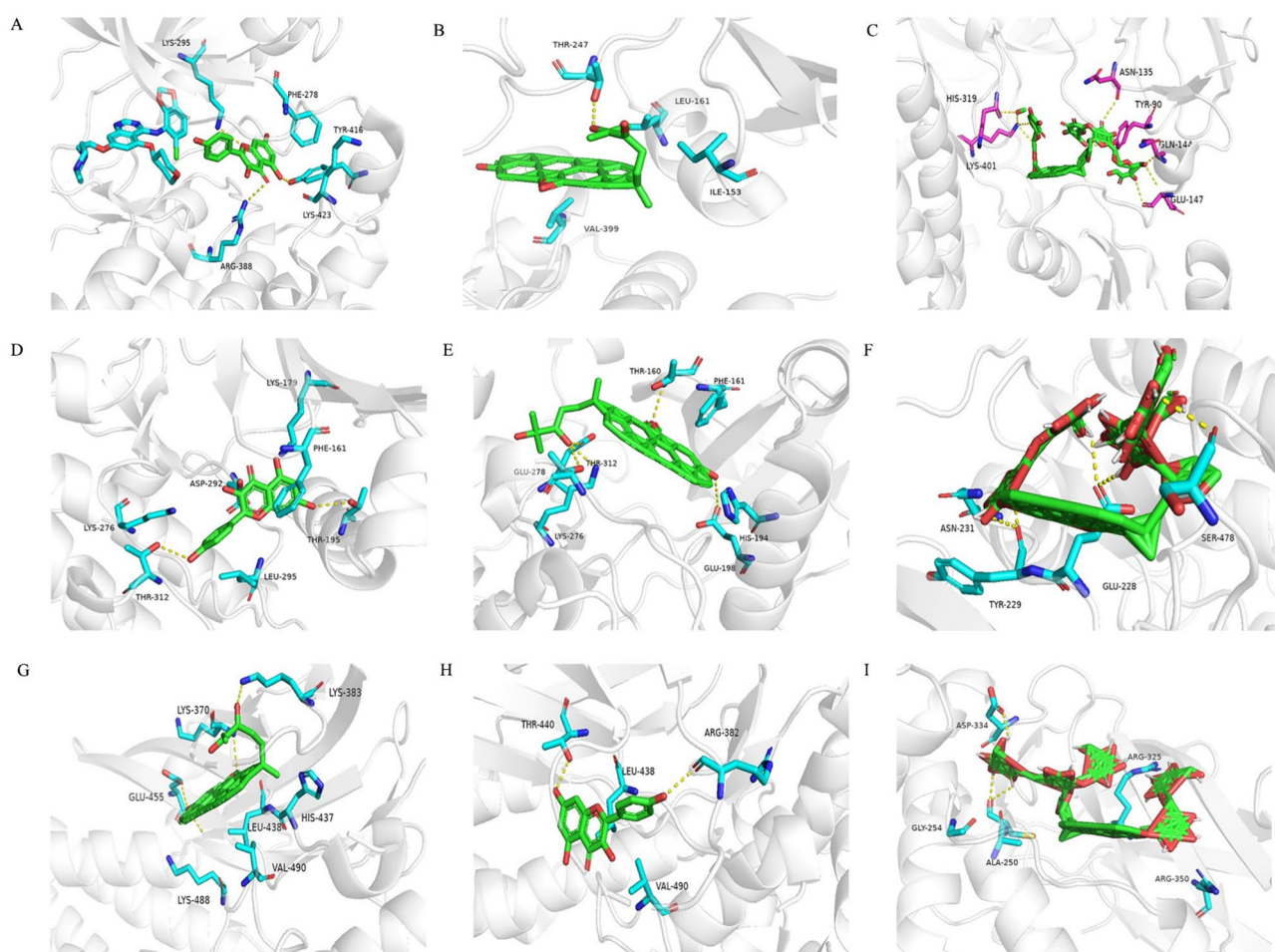


Fig. 5. Molecular docking visualization of LHG active compounds bound to key target proteins. (A) Binding mode of SRC with kaempferol. (B) Binding mode of SRC with Mogrol. (C) Binding mode of SRC with 11-oxomogroside V. (D) Binding mode of AKT1 with kaempferol. (E) Binding mode of AKT1 with Mogrol. (F) Binding mode of AKT1 with 11-oxomogroside V. (G) Binding mode of STAT3 with Mogrol. (H) Binding mode of STAT3 with kaempferol. (I) Binding mode of STAT3 with 11-oxomogroside V.

Protein	Grid_size	Docking score (kcal/mol)		
		Kaempferol	Mogrol	11-oxomogroside V
AKT1	47.25 × 47.25 × 47.25	-8.3	-9.5	-8.7
STAT3	78 × 98 × 88	-6.8	-8.7	-9.1
SRC	47.25 × 47.25 × 47.25	-8.6	-9.5	-11.0

Table 1. The docking scores.

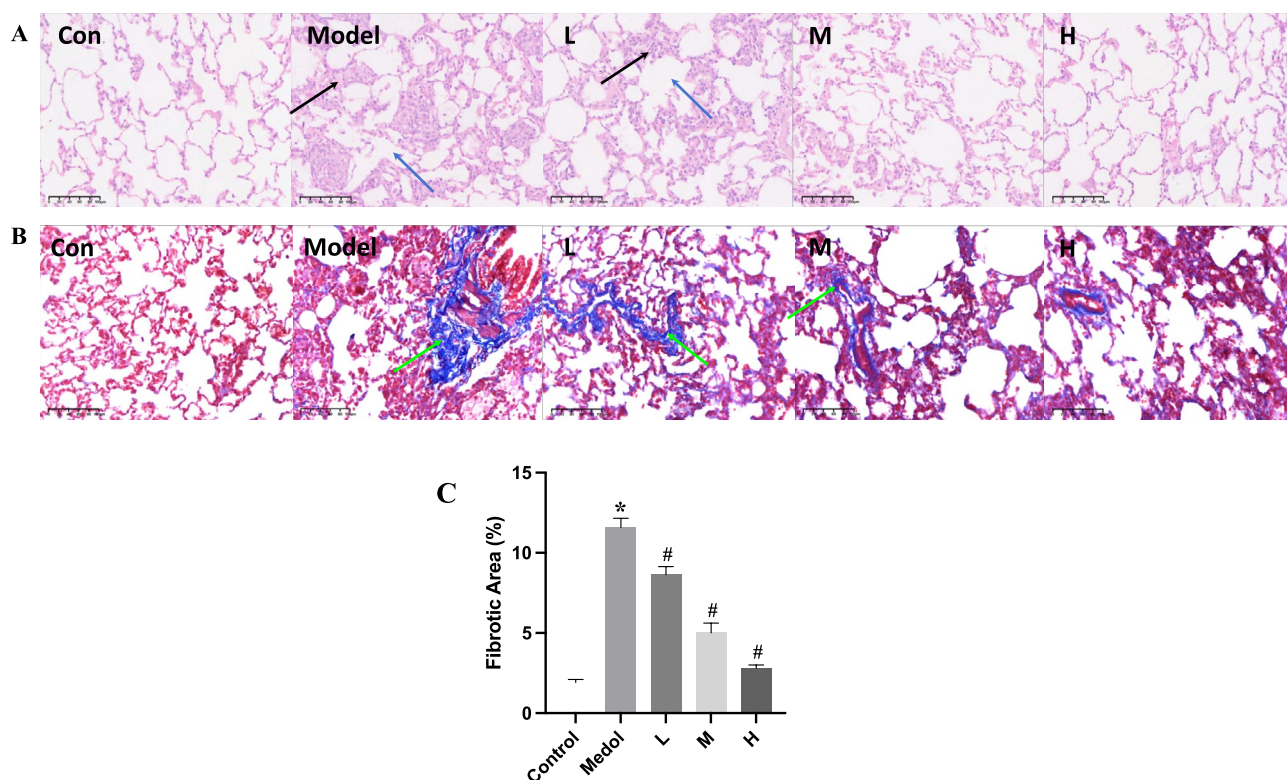


Fig. 6. the alleviating effect of LHG on BLM-induced PF. (A) Hematoxylin–eosin staining, magnified 200×, black arrows: inflammatory cell, blue arrow: alveolar fusion. (B) Fibrotic changes in the lung tissue of various groups of rats, magnified 200×, green arrows: collagen deposition. (C) Percentage of fibrotic area in lung tissue of rats in each group, where * $p < 0.05$ denotes statistical significance compared with the control group, and # $p < 0.05$ indicates significance compared with the model group.

hydrogen bonds formed with residues Lys179, Thr195, and Thr312, whereas residues Lys276, Leu295, Asp292, and Phe161 showed hydrophobic interactions (Fig. 5D). For AKT1 and Mogrol, hydrogen bonds were identified with Lys276, Glu198, Thr160, and Glu278, while His194 and Phe161 exhibited hydrophobic interactions (Fig. 5E). The docking analysis of AKT1 with 11-oxomogroside V (Fig. 5F) revealed hydrogen bonding with Ser478, Glu228, Tyr229, and Asn231. The docking of STAT3 with Mogrol (Fig. 5G) showed hydrogen bonds with Glu455, Lys383, and Lys370, as well as amino acid residues Lys488, Val490, Leu438, and His437 form hydrophobic interactions with Mogrol. The interaction between STAT3 and Kaempferol (Fig. 5H) highlighted hydrogen bonding with Thr440 and Arg382, while Leu438 and Val490 displayed hydrophobic interactions. STAT3 docking with 11-oxomogroside V (Fig. 5I) revealed hydrogen bonds with Asp334, Ala250, and Arg325, and hydrophobic interactions with Gly254 and Arg350. Lower binding energies indicate greater affinities between the receptor and ligand, with all binding energies below -6.8 kJ/mol (Table 1). These results suggest that the active components of LHG (Kaempferol, 11-oxomogroside V, and Mogrol) may bind to AKT1, SRC, and STAT3 to exert anti-IPF effects. (Fig. 6).

LHG alleviates BLM-induced IPF in rats

We investigated the therapeutic effects of LHG on pulmonary fibrosis by establishing a rat model of PF. Rats were administered LHG for 14 consecutive days. As shown in Fig. 6, the BLM-exposed group exhibited inflammatory cell infiltration, disruption of alveolar architecture, and thickening of the alveolar walls, whereas these pathological changes were ameliorated to varying degrees following LHG treatment at different dosages. Furthermore, BLM exposure resulted in a marked increase in collagen deposition within the lung tissues, while

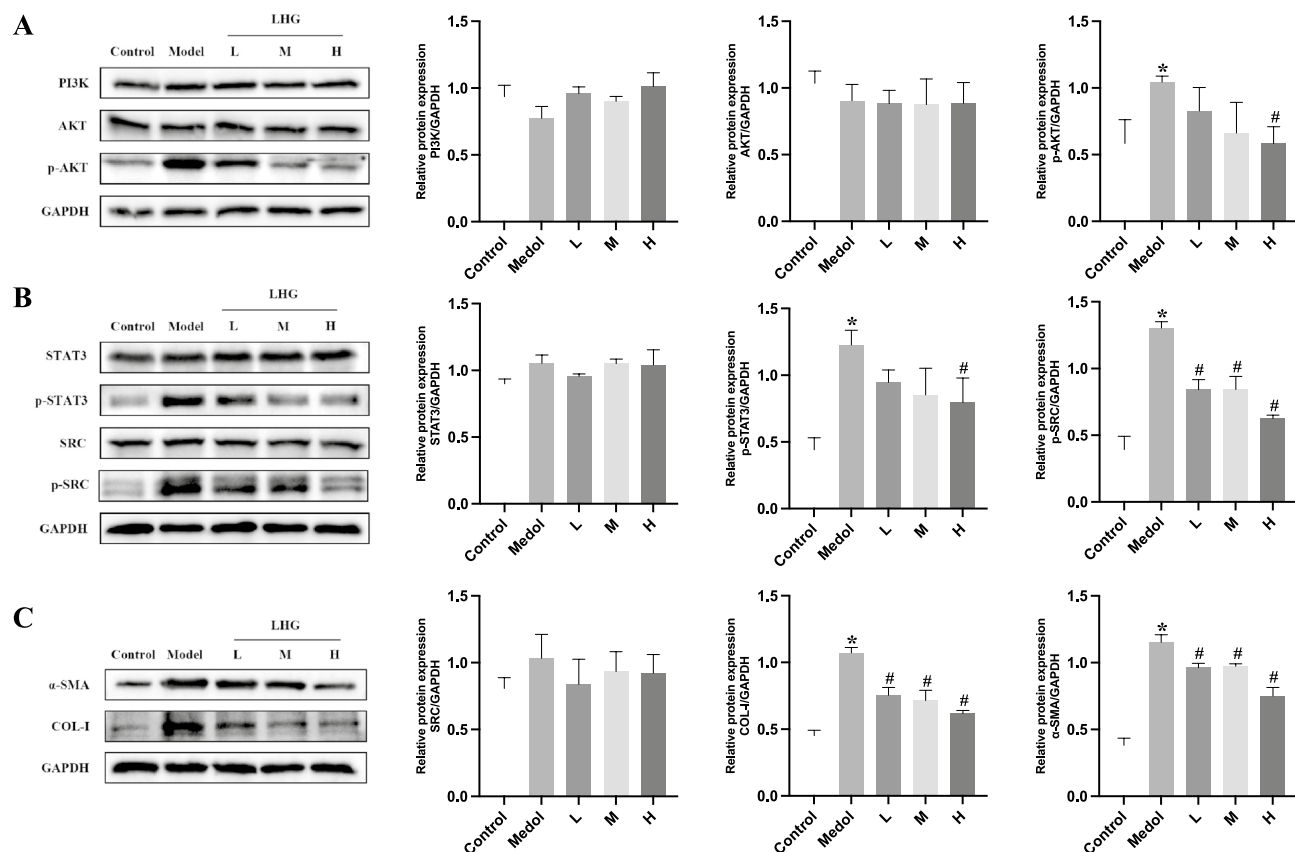


Fig. 7. the effects of LHG on the PI3K/AKT and STAT3/SRC pathways in rat lung tissues. **(A)** The expression levels and relative quantification of proteins involved in the PI3K/AKT signaling pathway across different experimental groups. **(B)** The proteins expression levels of the SRC/STAT3 signaling pathway across different experimental groups. **(C)** The Protein expression levels of fibrosis markers in each group. Statistical significance is indicated by * $p < 0.05$ compared with the control group, and # $p < 0.05$ compared with the model group.

this effect was significantly attenuated after LHG administration. These findings suggest that LHG treatment may inhibit BLM-induced pulmonary fibrosis in rats.

LHG inhibits rat lung fibrosis through PI3K/AKT and SRC/STAT3 pathways

LHG appears to inhibit pulmonary fibrosis in rats through suppression of the PI3K/AKT and SRC/STAT3 pathways. Network pharmacology analyses identified AKT, STAT3, and SRC as potential key targets of the active components of LHG, which are associated with its antifibrotic effects. To verify the role of LHG in mitigating BLM-induced pulmonary fibrosis in rats, we conducted Western blot analysis to assess the expression of these key targets. The results revealed that BLM induction significantly upregulated the expression of phosphorylated forms of these targets, including p-AKT, p-STAT3, and p-SRC. In contrast, increasing concentrations of LHG significantly suppressed the phosphorylation of AKT, STAT3, and SRC (Fig. 7A and B). Additionally, Western blot analysis (Fig. 7C) revealed elevated levels of fibrotic markers like α -smooth muscle actin (α -SMA) and collagen type I (Col-I) in the lungs of BLM-treated rats compared to the control group. However, α -SMA and Col-I levels were significantly reduced in the LHG-treated groups in a dose-dependent way. These *in vivo* findings indicate that LHG may attenuate BLM-induced pulmonary fibrosis in rats by modulating the PI3K/AKT and SRC/STAT3 pathways.

Discussion

Idiopathic pulmonary fibrosis (IPF) is a chronic, progressively worsening lung disease characterized by the buildup of fibrous tissue in the lung interstitium. This disease is confined to the lungs and is characterized by dyspnea and progressive deterioration of lung function, often associated with a poor prognosis²⁰. The pathogenesis of IPF is complex and remains largely unknown, and effective treatment options are still lacking. Consequently, IPF poses a significant health threat, contributing to increased morbidity and mortality rates globally and imposing a substantial burden on public health and medical resources. While novel therapeutics such as nintedanil and pirfenidone have demonstrated efficacy in ameliorating IPF symptoms, they are associated with various adverse effects, complications, and limited patient tolerability⁷. Luo Han Guo (LHG) contains a variety of bioactive constituents, including triterpenoids, flavonoids, and polysaccharides, which have demonstrated diverse pharmacological properties such as antitussive, antiasthmatic, antioxidant, hepatoprotective, hypoglycemic,

immunomodulatory, and antitumor effects⁹. Therefore, traditional Chinese medicine, exemplified by LHG, may present a promising option.

Network pharmacology employs high-throughput omics data analysis, computer simulations, and network database searches to study the multi-target networks of diseases caused by the actions of compounds²¹. Network pharmacology provides a robust framework for elucidating the mechanisms underlying pharmacological effects. Particularly in the study of herbal bioactive compounds, the advancement of network pharmacology has unveiled novel perspectives for identifying and understanding the complex bioactive ingredients within numerous Chinese herbs²². In this experiment, the application of network pharmacology addressed the limitations of traditional single-target research by predicting mechanisms across multiple dimensions. Specifically, this study constructed a “compound-target-pathway” network using network pharmacology. It revealed that bioactive compounds in *Siraitia grosvenorii* (such as kaempferol and mogroside V) exert anti-fibrotic effects through multiple pathways, including PI3K/AKT and SRC/STAT3. This demonstrates their comprehensive actions in suppressing inflammation, modulating cellular signaling, and regulating matrix metabolism. The “compound-target-pathway” network visually illustrates the synergistic mechanisms of multi-component interactions. Meanwhile, in vivo and in vitro experiments supplemented dynamic processes (e.g., changes in target activity during IPF progression). The integration of both approaches holistically elucidates the integrated anti-fibrotic effects of LHG. Furthermore, network pharmacology enables high-throughput target screening to narrow the scope for experimental validation. Through cross-database analysis (Venny 2.1), 91 overlapping targets were identified from potential targets of LHG and IPF-related genes. Core targets were further pinpointed via a protein–protein interaction (PPI) network. This process significantly reduced experimental randomness and enhanced research efficiency.

Our analysis revealed that 13 active compounds in LHG correspond to 430 targets. From these, we identified the top 100 critical targets and constructed a PPI network, which included AKT1, SRC, and STAT3. By analyzing the compound-target network diagrams of LHG active ingredients and their corresponding targets, we identified Kaempferol, Mogrol, and 11-oxomogroside V as the most promising active compounds. Kaempferol, a flavonol present in various natural products, exhibits multiple pharmacological activities, including anti-inflammatory, antioxidant, antitumor, and antifibrotic effects, and is currently employed in cancer chemotherapy²³. In animal models of silicosis, kaempferol administration significantly reduced lung inflammation within 7 days and inhibited silica-induced pulmonary fibrosis following 28 days of treatment²⁴. Additionally, Wang et al. demonstrated that kaempferol significantly inhibits non-small cell lung cancer (NSCLC) cell proliferation, promotes autophagy, and induces cell death by suppressing the PI3K/AKT/mTOR signaling pathway²⁵. Yan et al. found that kaempferol, in combination with lignans from the Renshen Pingfei Formula (RPF), exerted anti-IPF effects by targeting the AMPK/PPAR- γ signaling pathway, thereby inhibiting fibroblast proliferation and myofibroblast differentiation²⁶. Mogrol, a polyhydroxy compound derived from LHG extract, exhibits anti-inflammatory, antioxidant, antitumor, and antidiabetic properties, along with protective effects on various organs, such as the lungs and colon. He Li and colleagues reported that Mogrol inhibits lung cancer cell proliferation by activating the AMPK signaling pathway, inducing excessive autophagy and autophagic cell death, and activating the p53 pathway, leading to cell cycle arrest and apoptosis²⁷. Mogrol also attenuates colonic injury via the AMPK and NF- κ B signaling pathways²⁸. Moreover, Mogrol has demonstrated potential therapeutic effects on leukemia by inhibiting cell growth through suppression of the ERK1/2 and STAT3 pathways, leading to apoptosis in K562 cells²⁹. 11-oxomogroside V, a low-polarity rosmarinic glycoside isolated from LHG extract, regulates insulin secretion in type 2 diabetic rats via GLP-1 and exhibits antihyperglycemic effects³⁰. Additional studies have suggested that Flazin, another active component of LHG, may act as an activator of the Nrf2 pathway, enhancing NQO1, GSTP, and GSH protein expression, thereby preventing oxidative damage³¹. Similarly, 11-oxomogroside II A1 has been found to inhibit 12-O-tetradecanoylphorbol-13-acetate (TPA)-induced Epstein-Barr virus (EBV) early antigen activation³². Mogroside V reduces the inflammatory response of porcine alveolar macrophages via its antioxidant properties³³. Despite the diverse biological activities of LHG's active components, few studies have specifically examined their roles in alleviating the pathological processes of IPF, and the precise mechanisms of action remain unclear.

Therefore, we further analyzed 720 genes associated with the pathogenesis of IPF. GO and KEGG enrichment analyses, along with PPI networks constructed from disease-related targets, identified several key targets, including TNF, AKT1, SRC, and STAT3, which are primarily involved in the cancer pathway, PI3K-Akt signaling pathway, and EGFR tyrosine kinase inhibitor resistance.

We then performed a comprehensive analysis of the targets corresponding to 13 compounds of LHG and the intersection targets of IPF-related genes. The PPI network revealed 91 common targets interacting with each other, from which we identified 20 key targets. Among these, AKT1 is a pivotal protein kinase implicated in regulating apoptosis in alveolar macrophages through mediating mitochondrial autophagy, a process closely related to the development of pulmonary fibrosis³⁴. The EGFR/AKT signaling pathway is known to mediate fibroblast activation, a critical pathological process in IPF progression³⁵. Recent findings by Shuang Wang et al. indicated that inhibition of AKT1 activation suppresses cell cycle progression, resulting in tumor suppression in LUAD cells³⁶. SRC is considered a critical anti-IPF target; for example, the selective SRC kinase inhibitor Saracatinib has been shown to ameliorate fibrotic symptoms, including epithelial-mesenchymal transition and extracellular matrix accumulation³⁷. STAT3 is a transcription factor regulating fibroblast function in IPF³⁸, recent research has shown that hesperidin reduces BLM-induced lung fibrosis in mice through the IL6/STAT3 signaling pathway, possibly influencing fibroblast senescence³⁹. SRC functions as an upstream kinase of STAT3, and the SRC/STAT3 signaling pathway is thought to have anti-IPF effects. Li et al. reported that arginine deficiency and arginine deaminase treatment mitigated bleomycin-induced pulmonary fibrosis in mice, with the SRC/STAT3 signaling pathway playing a significant role in this process⁴⁰. KEGG pathway and GO enrichment analyses indicated that the intersecting targets were primarily associated with cancer pathways, EGFR tyrosine

kinase inhibitor resistance, TNF signaling pathway, and PI3K/AKT signaling pathway. These findings suggest that LHG may alleviate IPF by modulating processes such as extracellular matrix deposition, response to exogenous stimuli, and inflammation. Notably, the activation of both the PI3K-Akt and MAPK signaling pathways to bypass EGFR off-target effects, as well as the activation of the EGFR/SRC/STAT3 signaling axis, has been implicated in sorafenib resistance, which is closely linked to EGFR tyrosine kinase inhibitor resistance^{41,42}.

Taken together, we identified that AKT1, SRC, and STAT3 serve as pivotal targets for the active components of LHG and are also key genes involved in the pathogenesis of IPF. These targets play essential roles in both the protein interaction network of LHG targets and the protein interaction network of intersecting targets, where the physiological processes and pathways regulated by LHG are similar to those enriched in IPF-related genes. Furthermore, molecular docking studies indicated a mean binding affinity of -8.9 kcal/mol between LHG's active ingredients and key target proteins, demonstrating strong binding interactions. Therefore, we propose that AKT1, SRC, and STAT3 represent critical therapeutic targets of LHG in the treatment of IPF, closely linked to its pharmacological effects.

To validate the *in vivo* efficacy of LHG, we established a BLM-induced pulmonary fibrosis model in animals. Pathological changes in lung tissue were examined, alongside the expression of key signaling proteins and fibrosis markers, such as α -SMA and Col-I⁴³. Histopathological analysis revealed that LHG significantly ameliorated lung tissue architecture compared to the model group, with reductions in alveolar wall thickening, alleviation of lung injury, and attenuation of collagen deposition in a dose-dependent manner following LHG treatment.

Moreover, levels of phosphorylated forms of AKT, SRC, and STAT3 were significantly decreased in response to LHG treatment, and this effect was inversely proportional to the administered dose. Similarly, fibrosis markers α -SMA and Col-I exhibited the same trend. These results indicate that LHG mitigates IPF by reducing collagen buildup through modulation of the PI3K/AKT and SRC/STAT3 pathways. Previous studies have shown Kaempferol, a key active compound in the Qingzaojiufei Decoction, binds effectively to AKT1 and exerts antifibrotic effects on the lungs⁴⁴. Additionally, Kaempferol has been demonstrated to exert antitumor effects by inhibiting the EGFR/SRC/STAT3 signaling pathway⁴⁵ and to reduce triglyceride accumulation by suppressing AKT expression⁴⁶. However, to date, no literature has reported that LHG or its active components, such as Mogrol and 11-oxomogrosin V, directly target the AKT or SRC/STAT3 pathways in IPF. The present study, therefore, predicts the interactions between LHG's active ingredients and these critical signaling pathways. Further investigation is needed to fully understand the mechanisms through which LHG's active compounds target AKT, SRC, and STAT3 in IPF.

Presently, network pharmacology is advancing toward a model that integrates computational, experimental, and clinical research⁴⁷. To enhance the accuracy and reliability of our findings, this study combined network pharmacology with *in vivo* experimental approaches. The investigation was conducted in three stages to predict the pharmacological mechanisms of LHG. First, we identified the active ingredients and their corresponding targets using authoritative databases, constructed PPI networks and compound-target maps for key targets, and conducted functional enrichment analysis. Second, we screened and performed a functional analysis of IPF-related target genes, preliminarily identifying key genes. Finally, we conducted a PPI analysis of the cross-targets between LHG's active ingredients and IPF-related genes and performed cross-target enrichment analysis to further refine the predicted results.

To verify and strengthen the reliability of our predictions from the network pharmacology approach, we applied molecular docking simulations to assess the binding affinity between LHG's active ingredients and key target proteins. These findings were validated through *in vivo* experiments, confirming the involvement of the predicted targets and signaling pathways in LHG's treatment of IPF, thus providing a robust theoretical foundation for future anti-IPF pharmacological studies. Nevertheless, several areas warrant further investigation. First, serum medicinal chemistry could be utilized to analyze the composition of active compounds in serum following LHG administration, potentially yielding insights into the directly bioactive constituents. Second, the precise mechanisms by which individual active ingredients exert their effects could be elucidated through further *in vitro* studies.

However, the application of network pharmacology has limitations requiring improvement. For example, although this study reduced prediction bias through dual validation via molecular docking (binding energy verification) and animal experiments (protein expression detection), the potential impact of database coverage on results must be acknowledged. Furthermore, network pharmacology relies on static data modeling, which cannot reflect the temporal changes in target activity during IPF progression or simulate the absorption, distribution, metabolism, and excretion (ADME) processes of Luo Han Guo components *in vivo*.

In conclusion, this study demonstrates that LHG reduces extracellular matrix collagen deposition by regulating the PI3K/AKT and SRC/STAT3 signaling pathways, thereby ameliorating PF. The results indicate that LHG may offer a promising novel treatment strategy for PF, providing a strong theoretical and experimental foundation for future pharmacological research.

Data availability

The data obtained in this study are available from the corresponding author upon reasonable request.

Received: 29 November 2024; Accepted: 20 October 2025

Published online: 21 November 2025

References

1. Liu, G. Y., Budinger, G. R. S. & Dematte, J. E. Advances in the management of idiopathic pulmonary fibrosis and progressive pulmonary fibrosis. *BMJ* **377**, e066354 (2022).
2. Richeldi, L., Collard, H. R. & Jones, M. G. Idiopathic pulmonary fibrosis. *Lancet* **389**, 1941–1952 (2017).

3. Fernández Pérez, E. R. et al. Incidence, prevalence, and clinical course of idiopathic pulmonary fibrosis: A population-based study. *Chest* **137**, 129–137 (2010).
4. Phan, T. H. G. et al. Emerging cellular and molecular determinants of idiopathic pulmonary fibrosis. *Cell Mol Life Sci* **78**, 2031–2057 (2021).
5. Rochweg, B. et al. Treatment of idiopathic pulmonary fibrosis: A network meta-analysis. *BMC Med* **14**, 18 (2016).
6. West, A. et al. Inhaled pirfenidone solution (AP01) for IPF: a randomised, open-label, dose-response trial. *Thorax* **78**, 882–889 (2023).
7. Galli, J. A. et al. Pirfenidone and nintedanib for pulmonary fibrosis in clinical practice : Tolerability and adverse drug reactions. *Respirology (Carlton Vic)*. **22**, 1171–1178 (2017).
8. Duan, J. et al. *Siraitia grosvenorii* (Swingle) C Jeffrey : Research progress of its active components, pharmacological effects, and extraction method s. *Foods*. **12**, 1373 (2023).
9. Li, C. et al. Chemistry and pharmacology of *Siraitia grosvenorii*: A review. *Chin J Nat Med* **12**, 89–102 (2014).
10. Liu, H., Wang, C., Qi, X., Zou, J. & Sun, Z. Antiglycation and antioxidant activities of mogroside extract from *Siraitia grosvenorii* (Swingle) fruits. *J. Food Sci. Technol.* **55**, 1880–1888 (2018).
11. Chen, G. et al. Neuroprotective effect of mogrol against $A\beta_{1-42}$ -induced memory impairment neuroinflammation and apoptosis in mice. *J. Pharm Pharmacol.* **71**, 869–877 (2019).
12. Abdel-Hamid, M. et al. Bioactive properties of probiotic set-yogurt supplemented with *Siraitia grosvenorii* fruit extract. *Food Chem* **303**, 125400 (2020).
13. Kim, M.-S. et al. *Siraitia grosvenorii* extract attenuates airway inflammation in a murine model of chronic obstructive pulmonary disease induced by cigarette smoke and lipopolysaccharide. *Nutrients* **15**, 468 (2023).
14. Sung, Y.-Y. et al. *Siraitia grosvenorii* extract attenuates airway inflammation in a mouse model of respiratory disease induced by particulate matter 10 plus diesel exhaust particles. *Nutrients* **15**, 4140 (2023).
15. Jaiswal, V. & Lee, H. J. Pharmacological activities of mogrol: Potential phytochemical against different diseases. *Life* **13**, 555 (2023).
16. Sung, Y.-Y. et al. *Siraitia grosvenorii* residual extract attenuates ovalbumin-induced lung inflammation by down-regulating IL-4, IL-5, IL-13, IL-17, and MUC5AC expression in mice. *Phytomedicine* **61**, 152835 (2019).
17. Hopkins, A. L. Network pharmacology: The next paradigm in drug discovery. *Nat Chem Biol* **4**, 682–690 (2008).
18. Zhang, R., Zhu, X., Bai, H. & Ning, K. Network pharmacology databases for traditional Chinese medicine: Review and assessment. *Front. Pharmacol.* **10**, 123 (2019).
19. Aucar, M. G. & Cavasotto, C. N. Molecular docking using quantum mechanical-based methods. *Methods Mol. Biol.* **2114**, 269–284 (2020).
20. Raghu, G. et al. An official ATS/ERS/JRS/ALAT statement: idiopathic pulmonary fibrosis: Evidence-based guidelines for diagnosis and management. *Am. J. Respir. Crit. Care Med.* **183**, 788–824 (2011).
21. Song, F. et al. Uncovering the mechanism of Kang-ai injection for treating intrahepatic cholangiocarcinoma based on network pharmacology, molecular docking, and *in vitro* validation. *Front Pharmacol.* **14**, 1129709 (2023).
22. Lai, X. et al. Editorial: Network pharmacology and traditional medicine. *Front Pharmacol.* **11**, 1194 (2020).
23. Imran, M. et al. Kaempferol: A key emphasis to its anticancer potential. *Molecules* **24**, 2277 (2019).
24. Liu, H. et al. Kaempferol modulates autophagy and alleviates silica-induced pulmonary fibrosis. *DNA Cell Biol.* **38**, 1418–1426 (2019).
25. Wang, R. et al. Kaempferol promotes non-small cell lung cancer cell autophagy via restricting Met pathway. *Phytomedicine* **121**, 155090 (2023).
26. Yan, L., Jiang, M.-Y. & Fan, X.-S. Research into the anti-pulmonary fibrosis mechanism of Renshen Pingfei formula based on network pharmacology, metabolomics, and verification of AMPK/PPAR- γ pathway of active ingredients. *J. Ethnopharmacol.* **317**, 116773 (2023).
27. Li, H. et al. Mogrol suppresses lung cancer cell growth by activating AMPK-dependent autophagic death and inducing p53-dependent cell cycle arrest and apoptosis. *Toxicol Appl Pharmacol* **444**, 116037 (2022).
28. Liang, H. et al. Mogrol, an aglycone of mogrosides, attenuates ulcerative colitis by promoting AMPK activation. *Phytomedicine* **81**, 153427 (2021).
29. Liu, C. et al. Mogrol represents a novel leukemia therapeutic, via ERK and STAT3 inhibition. *Am. J. Cancer Res.* **5**, 1308–1318 (2015).
30. Zhang, Y., Zhou, G., Peng, Y., Wang, M. & Li, X. Anti-hyperglycemic and anti-hyperlipidemic effects of a special fraction of Luohanguo extract on obese T2DM rats. *J. Ethnopharmacol.* **247**, 112273 (2020).
31. Fuda, H. et al. Flazin as a promising Nrf2 pathway activator. *J. Agric. Food Chem.* **67**, 12844–12853 (2019).
32. Akihisa, T. et al. Cucurbitane glycosides from the fruits of *Siraitia grosvenorii* and their inhibitory effects on Epstein-Barr virus activation. *J. Nat. Prod.* **70**, 783–788 (2007).
33. Shen, J. et al. Mogroside V exerts anti-inflammatory effects on fine particulate matter-induced inflammation in porcine alveolar macrophages. *Toxicol. In Vitro* **80**, 105326 (2022).
34. Larson-Casey, J. L., Deshane, J. S., Ryan, A. J., Thannickal, V. J. & Carter, A. B. Macrophage Akt1 kinase-mediated mitophagy modulates apoptosis resistance and pulmonary fibrosis. *Immunity* **44**, 582–596 (2016).
35. Wang, N. et al. LncRNA LPAL2/miR-1287-5p/EGFR axis modulates TED-derived orbital fibroblast activation through cell adhesion factors. *J. Clin. Endocrinol. Metab.* **106**, e2866–e2886 (2021).
36. Wang, S. et al. PKMYT1 inhibits lung adenocarcinoma progression by abrogating AKT1 activity. *Cell Oncol. (Dordr)* **46**, 195–209 (2023).
37. Ahangari, F. et al. Saracatinib, a selective src kinase inhibitor, blocks fibrotic responses in preclinical models of pulmonary fibrosis. *Am. J. Respir. Crit. Care Med.* **206**, 1463–1479 (2022).
38. Pechkovsky, D. V. et al. STAT3-mediated signaling dysregulates lung fibroblast-myofibroblast activation and differentiation in UIP/IPF. *Am. J. Pathol.* **180**, 1398–1412 (2012).
39. Han, D. et al. Hesperidin inhibits lung fibroblast senescence via IL-6/STAT3 signaling pathway to suppress pulmonary fibrosis. *Phytomedicine* **112**, 154680 (2023).
40. Li, J.-M. et al. Therapeutic targeting of argininosuccinate synthase 1 (ASS1)-deficient pulmonary fibrosis. *Mol. Ther.* **29**, 1487–1500 (2021).
41. Bertoli, E. et al. Acquired resistance to osimertinib in EGFR-mutated non-small cell lung cancer: How do we overcome it?. *IJMS* **23**, 6936 (2022).
42. Li, R. et al. Secreted GRP78 activates EGFR-SRC-STAT3 signaling and confers the resistance to sorafenib in HCC cells. *Oncotarget* **8**, 19354–19364 (2017).
43. Ji, H. et al. Metformin attenuates fibroblast activation during pulmonary fibrosis by targeting S100A4 via AMPK-STAT3 axis. *Front. Pharmacol.* **14**, 1089812 (2023).
44. Zhao, Y. et al. Molecular mechanism of qingzaojiufei decoction in the treatment of pulmonary fibrosis based on network pharmacology and molecular docking. *Curr. Pharm. Des.* **29**, 2161–2176 (2023).
45. Zhou, J., Liu, Y., Chen, J., Xiong, N. & Yi, D. Kaempferol suppresses glioma progression and synergistically enhances the antitumor activity of gefitinib by inhibiting the EGFR/SRC/STAT3 signaling pathway. *Drug Dev. Res.* **84**, 592–610 (2023).
46. Hoang, M.-H., Jia, Y., Lee, J. H., Kim, Y. & Lee, S.-J. Kaempferol reduces hepatic triglyceride accumulation by inhibiting Akt. *J. Food Biochem.* **43**, e13034 (2019).

47. Wang, Z.-Y., Wang, X., Zhang, D.-Y., Hu, Y.-J. & Li, S. Traditional Chinese medicine network pharmacology: Development in new era under guidance of network pharmacology evaluation method guidance. *Zhongguo Zhong Yao Za Zhi* **47**, 7–17 (2022).

Author contributions

Qinlin Cui, Yingyi Liu: conceptualization, writing—Original Draft; Yuxuan Li, Zhan Li: validation, methodology; Wencai Wei, Simei Yang: methodology, formal analysis; Xin Liu, Lei Chen, Yihan Li: Data organization and verification; Kunyu Xu: resources, supervision; Qingbi Zhang, Jun Bai: writing—review & editing, funding acquisition; All authors have read and approved the manuscript.

Funding

This work was supported by the Scientific Fund of Luzhou city (2023JYJ011, 2024JYJ005); Fund Project of Southwest Medical University (2021ZKMS001, 2023QN115).

Declarations

Competing interests

The authors declare no competing interests.

Ethical approval

This study was approved by the Southwest Medical University committee (Permit SWMU20230078). This study complied with the Regulations on the Management of Laboratory Animals issued by the National Science. All procedures were performed in accordance with the ethical standards of the Guide for the Care and Use of Laboratory Animals published by the National Institutes of Health and ARRIVE guidelines.

Additional information

Supplementary Information The online version contains supplementary material available at <https://doi.org/10.1038/s41598-025-25270-3>.

Correspondence and requests for materials should be addressed to Q.Z. or J.B.

Reprints and permissions information is available at www.nature.com/reprints.

Publisher's note Springer Nature remains neutral with regard to jurisdictional claims in published maps and institutional affiliations.

Open Access This article is licensed under a Creative Commons Attribution-NonCommercial-NoDerivatives 4.0 International License, which permits any non-commercial use, sharing, distribution and reproduction in any medium or format, as long as you give appropriate credit to the original author(s) and the source, provide a link to the Creative Commons licence, and indicate if you modified the licensed material. You do not have permission under this licence to share adapted material derived from this article or parts of it. The images or other third party material in this article are included in the article's Creative Commons licence, unless indicated otherwise in a credit line to the material. If material is not included in the article's Creative Commons licence and your intended use is not permitted by statutory regulation or exceeds the permitted use, you will need to obtain permission directly from the copyright holder. To view a copy of this licence, visit <http://creativecommons.org/licenses/by-nc-nd/4.0/>.

© The Author(s) 2025